Computational Studies of the Locomotion of Dolphins and Sharks Using Smoothed Particle Hydrodynamics

R.C.Z. Cohen and P.W. Cleary

CSIRO Mathematics, Informatics & Statistics, Clayton, VIC, Australia

Abstract— **Many marine animals cruise efficiently within a small range of propulsive Strouhal numbers. More recently it has been proposed that optimal vortex formation is the underlying principle to this universal Strouhal number constraint. The computational fluid dynamics technique known as Smoothed Particle Hydrodynamics (SPH) is used to study the propulsion of high speed marine animals – the Bottlenose Dolphin and the White Pointer Shark. The thrust generation and corresponding vortical flow structures are considered in detail over a range of Strouhal numbers.**

Keywords— **Marine animal swimming, Smoothed particle hydrodynamics, Dolphins, Sharks.**

I. Introduction

Characterization of an animal's swimming motion is typically made through the Strouhal number, $St = f A / u_\infty$, where f is the stroke frequency, A in the stroke peak-to-peak amplitude and u_∞ is the bulk animal speed. Research has shown that a number of animals including dolphins, sharks and fish swim in such a way as to achieve high propulsive efficiency [1]. These animals tend to swim in a narrow range of Strouhal numbers between 0.2 and 0.4 which implies dynamic similarity across species and an adherence to optimizing hydrodynamic phenomena. More recently it has been proposed that this Strouhal number constraint is actually a consequence of the condition for optimal vortex formation [2].

Dolphins appear to be "effortless" high speed swimmers with extremely low drag and high propulsion. This is in part due to their streamlined shape which optimizes the trade off between drag, volume and frontal area [3]. There is still debate as to whether special properties of the skin itself contribute to the drag reduction or whether it is simply due to the maintaining of an attached turbulent boundary layer.

Sharks are high speed thunniform swimmers. To compensate for the reduced buoyancy of their oil filled livers (rather than gas filled bladders), sharks have a light cartilaginous skeleton [4]. This gives them much greater flexibility than their bony counterparts including dolphins. Some species of shark have less buoyancy than their weight so must keep moving and utilize dynamic lift to maintain their depth. Unlike dolphins, sharks have dermal denticles on the leading edges of their fins and bodies to reduce the turbulent shear stress and the overall drag [5].

In this study, the analysis of submerged swimming was conducted for a Common Bottlenose Dolphin (Tursiops truncatus) and a Great White Shark (Carcharodon carcharias) over a range of propulsive Strouhal numbers. The relationship between the thrust generation, vortex formation and the propulsive Strouhal number is investigated. More generally, this work presents a robust framework for studying and comparing the dynamics of different swimming creatures.

II. Numerical method

A. Fluid Solver

The simulation of biological swimming presents a modeling challenge because of the rapidly deforming animal surface that is two-way coupled with the fluid. To avoid volume meshing difficulties, this study utilizes the Lagrangian mesh-free numerical method known as Smoothed Particle Hydrodynamics (SPH) [6-8]. The particles in this method represent discrete volumes in the continuum of the fluid and are free to advect around in response to the flow. The fluid state is stored with each of these particles, with interpolation and gradient calculations evaluated using kernel based functions. The interaction between the animal model and the discretized fluid is achieved through a realistic time-deforming surface mesh that imposes the boundary condition. The SPH method has previously been applied to human swimming of glide pose towing and dolphin kick which provides similar modeling challenges [9].

B. Marine Animal Geometries

Realistic surface meshes of an adult sized Great White Shark (Carcharodon carcharias) and Common Bottlenose Dolphin (Tursiops truncatus) were "rigged" to an underlying skeletal structure using the commercial software animation package Autodesk Maya [10]. This enables the surface to be articulated into any desired pose by manipulating the joints of the skeleton. Video footage of the motion of these animals was then used as a reference for animating their

C.T. Lim and J.C.H. Goh (Eds.): WCB 2010, IFMBE Proceedings 31, pp. 22–25, 2010.
www.springerlink.com

surface deformation, producing virtual animals performing swimming actions that are typical of straight line cruising.

The model for the dolphin is shown in Fig. 1. A simple spine based skeletal structure is adequate for a straight line swimming action. Each of the labeled joints except T_5 was given synchronized sinusoidal rotations about their transverse axes. The final tail joint T_5, which controls the tail fluke, has out of phase rotations to make the tail fluke appear more passive as seen in video footage.

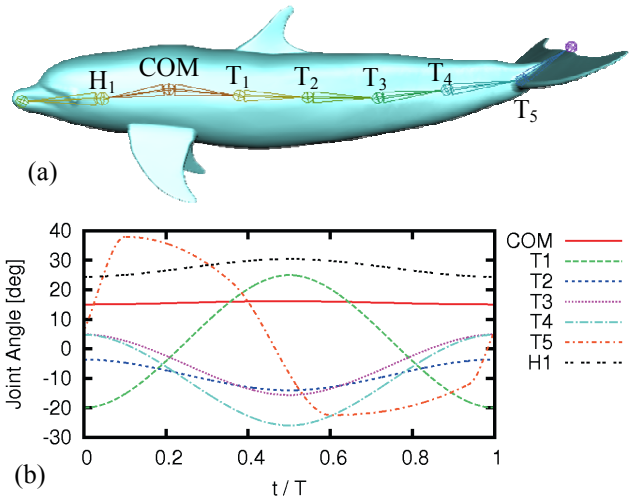

Fig. 1 Model for the bottlenose dolphin. (a) Surface mesh rigged with a skeletal structure. Only joints that rotate during the animation are labeled. (b) Joint orientations throughout the dolphin stroke cycle. The zero angle is with reference to the rigging pose which had the dolphin very curved

The model for the shark is given in Fig. 2. Unlike the dolphin, the shark's body undulations are about the vertical axis. For this straight line cruising thunniform motion, only the joints along the rear end of the shark had rotations applied to them. Joints T1, T2 and T3 had synchronized sinusoidal oscillations whilst the final joint, T_4 had out of phase oscillation to make the tail fin appear more passive.

The size of the dolphin and shark models used in this investigation are given in Table 1. The resultant peak-to-peak tail motion amplitudes are also given in this table. The simulations were conducted at the moderate depths of 1 m for the dolphin and 2 m for the much larger shark.

Table 1 Parameters of the dolphin and shark simulations

Parameter	Dolphin	Shark
Nose to tail length, L [m]	2.5	4
Volume [m^3]	0.152	0.667
Peak-to-peak tail amplitude, A [m]	1.148	1.26
Depth from free surface [m]	1	2

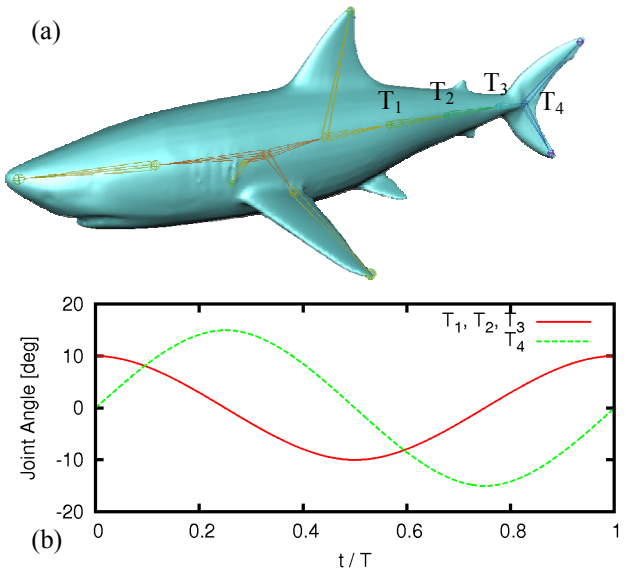

Fig. 2 Model for the white pointer shark. (a) Surface mesh rigged with a skeletal structure. Only joints that rotate during the animation are labeled. (b) Joint orientations throughout the shark stroke cycle

III. Results and Discussion

SPH simulation of the fluid moving around the dolphin and shark were performed using the animated surface meshes. The cases considered are given in Table 2. These cover a number of propulsive Strouhal numbers for both creatures. The minimum Strouhal numbers for each animal are within their most efficient propulsion regime [1].

Table 2 Simulation cases

Case name	Creature	Swim cycle frequency., $f = 1/T$ [Hz]	Swimming speed, u_∞ [m/s]	Propulsive Strouhal No. $St = fA / u_\infty$
D1	dolphin	1	2	0.57
D2	dolphin	1	3	0.38
D3	dolphin	2	2	1.15
D4	dolphin	2	3	0.77
S1	shark	1	4	0.32
S2	shark	2	4	0.63

A. *Bottlenose Dolphin*

The periodic oscillation of the dolphin's body produces similarly oscillatory thrust time histories, as can be seen in Fig 3. The higher frequency tail motion cases (D3 and D4) generate larger thrust. If two cases considered have identical frequencies, the case with a lower speed is observed to have

a larger net force. This is likely to be due to a reduction in drag force at the lower speed.

Fig. 4 shows a three-dimensional visualization of the coherent vortical flow structures produced by the low Strouhal number case D1. The up- and down-strokes of the tail generate hairpin type vortices which are initially joined but separate as they move downstream.

Instantaneous contours of spanwise vorticity of the fluid on vertical slices through the dolphin are shown in Fig. 5. This highlights the differences between the vortical structures of all the cases. The tail motion of the dolphin generates alternately signed spanwise vortices from the up and down strokes. The lower Strouhal number cases have more coherent wake structures which may be an indicator for more efficient propulsion.

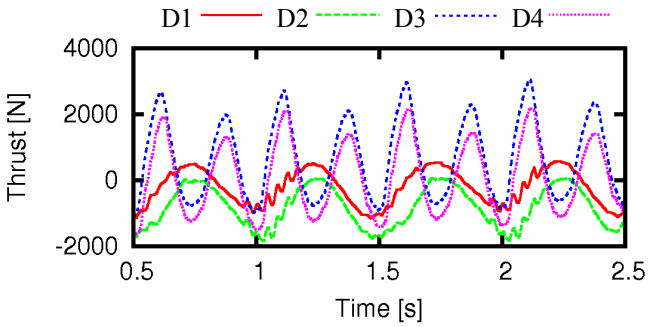

Fig. 3 Time histories of the thrust forces on the dolphin

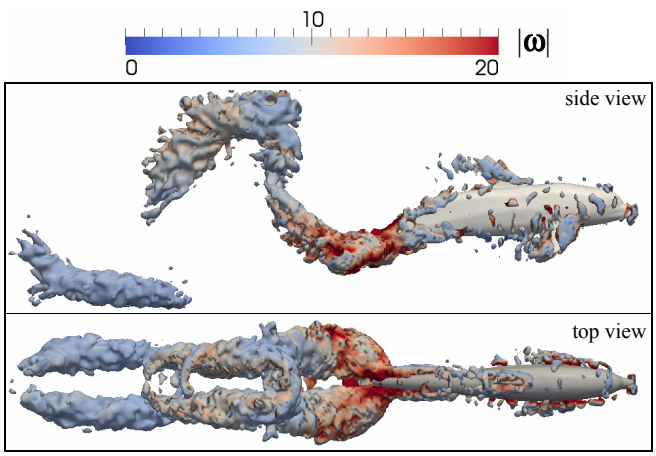

Fig. 4 Instantaneous three-dimensional vortical flow structures from dolphin flow simulations (case D1). These are isosurfaces of λ_2=0 colored by vorticity magnitude

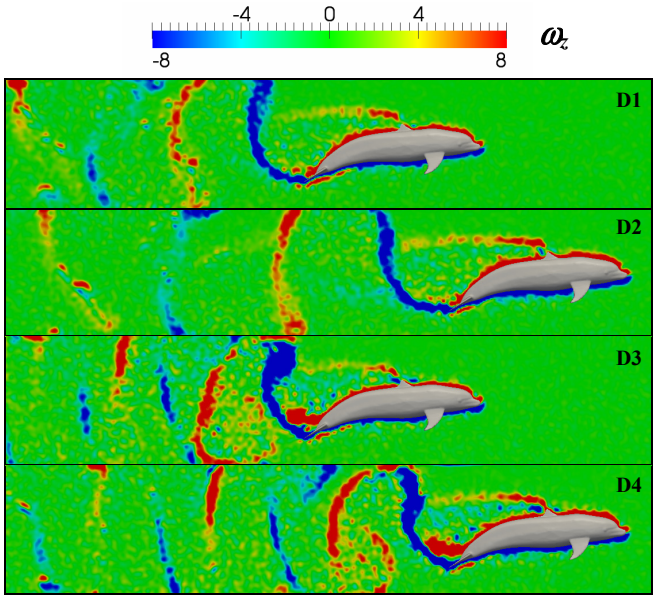

Fig. 5 Instantaneous contours of spanwise vorticity in the fluid on the vertical slice through the middle of the dolphin

B. White Pointer Shark

Figure 6 shows the thrust force time histories for the two shark cases. These are both oscillatory with the higher frequency case much more sinusoidal in shape. The amplitude of the force fluctuations are much larger in the higher frequency case S2 which is consistent with the dolphin study. Unlike the dolphin case, the shark does not experience a significant increase in mean force with the increase in stroke frequency. The magnitude of the drag force appears to be an over-prediction in these simulations. This is likely to be the result of not including any special treatment for the low resistance skin of the shark.

Visualizations of the three-dimensional vortical flow structures for the shark case S1 are shown in Fig. 7. Vortices are observed to roll up around the shark's nose and from the large fins. The motion of the tail fin generates vortical structures that are less coherent than in the dolphin case. These structures are also less symmetrical for the shark which has an asymmetrical tail.

The fluid vorticity is shown on a slice that passes through the shark in Fig. 8. Unsteadiness in the boundary layers appears to cause early flow separation which may explain the large drag forces. The alternately signed arrays of vortical flow structures are similar in appearance between the two cases. From case S1 to S2 the frequency doubles and the spacing between the vortical structures halves. They are being generated by the motion of the tail fin so the spacing between oppositely signed vortices in the wake is proportional to the stroke period.

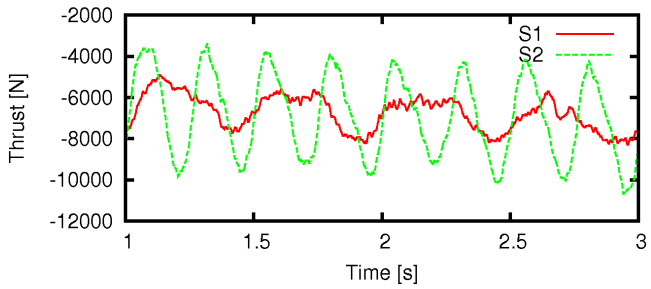

Fig. 6 Time histories of the thrust forces on the shark

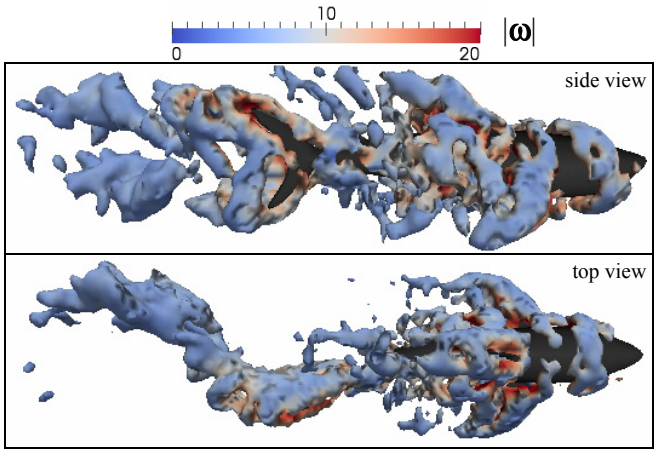

Fig. 7 Instantaneous three-dimensional vortical flow structures from shark flow simulations (case S1). These are isosurfaces of λ_2=0 colored by vorticity magnitude

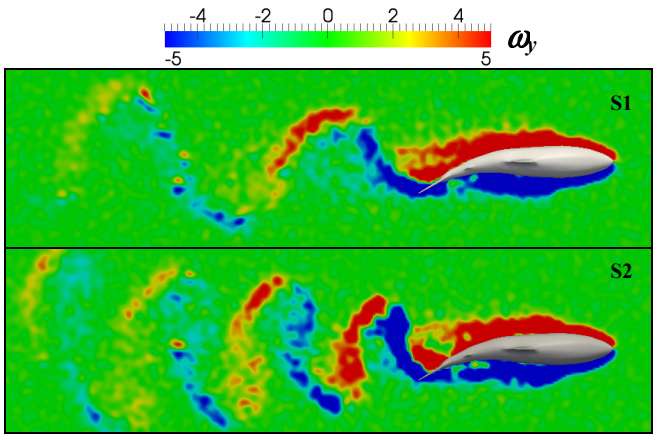

Fig. 8 Instantaneous contours of vertical vorticity in the fluid on the horizontal slice through the middle of the shark

IV. Conclusions

Investigations of animal and fish propulsion using computational fluid dynamics has the advantages of providing a controlled environment for studies without the difficulties of handling a live creature. Additionally, this provides detailed information about the flow field for analysis. Smoothed particle hydrodynamics has been demonstrated to be suitable for use in studying flows around the complex deforming shapes of marine animals.

In the present study two high speed marine animals, the Bottlenose Dolphin and White Pointer Shark were considered. Both use a rear tail fin to provide most of their propulsion. The results in the present study showed that strong alternately signed vortices are generated by the oscillatory motion of their tails. Three-dimensional visualizations of these vortical structures revealed their hairpin-like structure for the dolphin and a much less coherent wake structure for the shark. For the dolphin cases considered, net thrust increased with increases in tail motion frequency but this trend was not observed in the case of the shark.

Given the demonstrated feasibility of modeling marine animal swimming, these methods can be used to explore many questions about the quantitative sensitivity of propulsive efficiency to different stroke variations.

References

1. Taylor GK, Nudds RL, Thomas ALR (2003) Flying and swimming animals cruise at a Strouhal number tuned for high power efficiency. Nature 425:707-711.
2. Dabiri JO (2009) Optimal vortex formation as a unifying principle in biological propulsion. Ann Rev Fluid Mech 41:17–33.
3. Fish FE, Hui CA (1991) Dolphin swimming - a review. Mammal Rev 21:181-195.
4. Last PP, Stevens JD (2009) Sharks and rays of Australia. CSIRO Publishing, Melbourne.
5. Fish FE, Lauder GV (2006) Passive and active flow control by swimming fishes and mammals. Ann Rev Fluid Mech 38:193-224.
6. Monaghan JJ (1992) Smoothed Particle Hydrodynamics. Annu Rev Astron Astrophysics 30:543-574.
7. Monaghan JJ (1994) Simulating free surface flows with SPH. J Comput Phys 110:399-406.
8. Cleary PW (1998) Modelling confined multi-material heat and mass flows using SPH. Appl Math Model 22:981-993.
9. Cohen RCZ, Cleary PW, Mason B (2009) Simulations of human swimming using Smoothed Particle Hydrodynamics. In Proceedings of the Seventh International Conference on CFD in the Minerals and Process Industries, Melbourne, Australia, 2009.
10. Autodesk Maya 2008. http://usa.autodesk.com/

Author: Raymond Cohen
Institute: CSIRO Mathematics, Informatics & Statistics
Street: Gate 5, Normanby Road
City: Clayton
Country: Australia
Email: Raymond.Cohen@csiro